SCIENCE CHINA
Physics, Mechanics & Astronomy

• Research Paper •
Special Issue: Forward for the Department of Engineering Mechanics, Tsinghua University

April 2011 Vol.54 No.4: 675–682
doi: 10.1007/s11433-011-4269-1

Study of dynamic hydrophobicity of micro-structured hydrophobic surfaces and lotus leaves

HAO PengFei*, YAO ZhaoHui & ZHANG XiWen

Department of Engineering Mechanics, Tsinghua University, Beijing 100084, China

Received December 6, 2010; accepted January 6, 2011; published online February 14, 2011

The dynamic wetting characteristics of water droplets on silicon wafers with microscale regular pillars structures and fresh lotus leaves are investigated experimentally. We measured the static contact angle, contact angle hysteresis, and roll-off angle of water droplets on both of these superhydrophobic surfaces with a high speed contact angle meter. The dynamic contact angles and internal velocity distribution of water droplets on superhydrophobic surfaces were studied with a high-speed camera system and a particle image velocimetry (PIV) system, respectively. We found that the acceleration of water droplets when they slide off lotus leaves is greater than that of water droplets sliding off the silicon wafers with microscale pillar structures although the static contact angles of water droplets on lotus leaves are slightly smaller than those on the silicon wafers. The reason is that water droplets sliding off lotus leaves have smaller contact angle hysteresis and larger slip velocities. These results indicate that the dynamic contact angle hysteresis and sliding acceleration of liquid droplets are more suitable for reflecting the hydrophobicity of material surfaces compared with static contact angles. Our experiments also show that lotus leaves with multiscale micro/nanostructures have stronger hydrophobicity and self-cleaning properties compared with the micro-structured superhydrophobic surfaces.

droplet, hydrophobicity, contact angle, PIV

PACS: 47.55.np, 47.55.dr, 68.08.Bc

1 Introduction

The natural world has many examples of plants and animals with surfaces that have hydrophobic and self-cleaning properties [1,2]. For example, the surfaces of lotus leaves and rice leaves have droplet contact angles of over 150° and small roll-off angles (less than 5°). Barthlott and Neinhuis et al. [3] observed the microscopic structures of the leaf surfaces of plants and discovered that these hydrophobic and self-cleaning properties are brought about by both the micro/nano-scale hair-like structures on the leaf surface and the layer of wax crystals on these structures. Due to the potential applications and prospects of superhydrophobic surfaces in many fields, such as contamination prevention anti-icing, and microfluidics, the research on preparation technology of superhydrophobic surfaces and their wetting characteristics drew a lot of attention recently [4–7].

Research on surface physics and chemistry has shown that the micro/nano-structures and surfaces have a determining influence on the hydrophobicity of the surface. Regarding the effect of surface roughness on contact angles, Wenzel and Cassie et al. [8,9] proposed classical equations for the contact angles which involve the microscopic structures of the surface. Recently, research on the wetting characteristics of superhydrophobic surfaces has shown that contact angles are related not only to the solid area fractions of superhydrophobic surfaces, but also to the dimensions of the microscopic structures on rough surfaces and their geometrical topology [10,11]. Besides the static contact angle, contact angle hysteresis (the difference between the advancing angle and receding angle) and the roll-off angle

*Corresponding author (email: haopf@mail.tsinghua.edu.cn)

(the smallest angle of tilt that results in liquid droplets rolling off an inclined surface) are two other important parameters to evaluate the wettability of solid surfaces. As the contact angle hysteresis and roll-off angle of water droplets on superhydrophobic surfaces are relatively small, a slight disturbance will result in the droplet easily rolling off the solid surface; a few scholars have proposed models for predicting contact angle hysteresis and roll-off angles [12–14]. However, contact angle hysteresis and the roll-off angle are only apparent parameters, and are unable to provide the details of the sliding acceleration or velocity of the liquid droplets on superhydrophobic surfaces. Furthermore, a hydrophobic surface with a low sliding angle does not always exhibit high sliding acceleration or velocity for a water droplet [15–16]. Generally, the small contact angle hysteresis means that a liquid droplet can roll off easily due to the negligible static friction force. However, there are very few investigations on the dynamic contact angle and internal flow field while the water droplet is sliding on the superhydrophobic surface.

Suzuki et al. [17] evaluated the relationship between the sliding acceleration and the dynamic contact angle hysteresis of water droplets on a silicon surface that had been treated with fluoroalkylsilane. Song investigated the static and dynamic hydrophobicities of water droplets on a patterned surface prepared using fluoroalkylsilane with different molecular chain lengths. These results imply that the sliding acceleration of water droplets on hydrophobic surfaces is controllable by changing the pattern structure and its chemical composition [18]. Yoshida et al. [19] evaluated sliding acceleration of water droplets on several hydrophobic polymer coatings with smooth surfaces. Their results suggested that static and dynamic hydrophobicities were controllable by changing their molecular lengths and concentrations. At present, most of the researches on super hydrophobic properties are focused on the preparation technology of superhydrophobic materials, but there is still a need for more research on the wetting behavior of superhydrophobic materials, and fundamental problems such as which parameters are more suitable for judging the superhydrophobicity of a material. The comprehensive understanding of the dynamic contact angle and internal flow pattern of water droplets on microstructured superhydrophobic surfaces is still insufficient.

This article utilizes several experimental techniques to study the dynamic wetting characteristics of water droplets on silicon wafers with microscopic regular square cylindrical structures and fresh lotus leaves. We measured the static contact angle, contact angle hysteresis and roll-off angle of liquid droplets on both of these superhydrophobic surfaces, compared with the variation of the advancing and receding contact angles as liquid droplets slide off these two different superhydrophobic surfaces, and utilized particle image velocimetry (PIV) to measure the velocity distribution of liquid droplets on superhydrophobic surfaces.

2 Experimental section

2.1 Sample preparation

We utilized lithography and ion etching technology to treat silicon wafers with regular square cylindrical microstructures on their superhydrophobic surfaces with the square pillars (a = 4 μm). The pillars are uniformly distributed in a rectangular grid as shown in Figure 1. The area fractions f for four different samples are 0.04, 0.0625, 0.1111, and 0.16, where f is defined as $f = a^2/(a+s)^2$ and s is the spacing between the pillars. The first step in the sample preparation was the creation of a 350 μm thick 〈100〉 silicon wafer. Photolithography was then used to transfer the required pattern from a mask to the photoresist layer. The area that was not protected by the photoresist layer was etched with the ICP dry-etching method to finally create the roughness pattern on the wafer. A fixed pillar height (d = 35 μm) for all the pillar-structured surfaces studied was achieved by controlling the etching time. After the etching process, the remaining protective layers were removed from the silicon wafer. To make the silicon wafer hydrophobic, a monolayer of a hydrophobic substance was applied onto the surface; octadecyltrichlorosilane (OTS) of formula $C_{18}H_{37}Cl_3Si$ (Acros Organics) was used for this purpose. The surface was first treated with a solution of "Piranha", composed of 70% sulfuric acid (H_2SO_4) solution with 98% concentration

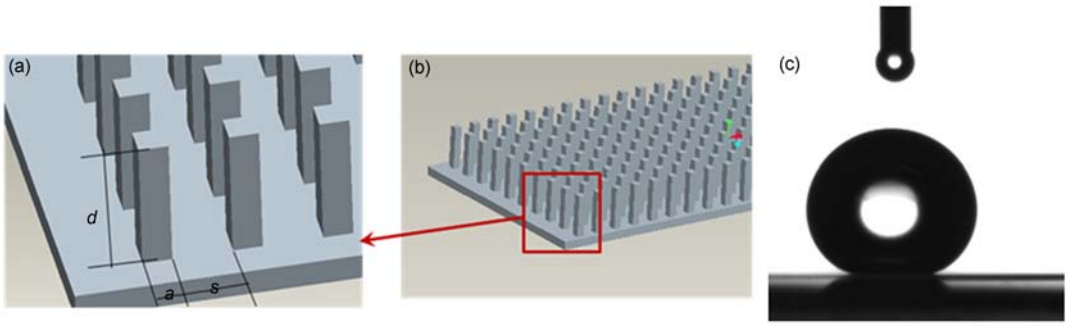

Figure 1 (a) and (b) Pillar-like microstructured surfaces; (c) a 10 μL water droplet on microstructured surfaces (a=4 μm, s=16 μm, f=0.04), CA=162°.

and 30% hydrogen peroxide (H_2O_2) solution with 20% concentration. The process consists of immersing the surface in the solution of "Piranha" and keeping it at a constant temperature of 90°C for 30 min inside a heater. The surface was then rinsed with deionized water and dried. In a completely dry container, 0.1 mL of OTS is mixed with 25 mL of hexadecane. The surface was rinsed with this new solution and baked in an oven for 20 min. Then the surface was treated with chloroform for 15 min to remove any dust, and finally the surface was soaked in anhydrous alcohol for 30 min and dried. After chemical modification, the Young's contact angle ϕ_0 was measured to be 105° on the smooth surface.

The apparent contact angle and sliding angle were measured with a commercial contact angle meter (OCAH200, Dataphysics, Germany). The mass of the water droplet used for the measurements was 10 μL. In order to achieve best precision, the contact angles were measured at five different points for each sample, the mean of the measured values was used as the contact angle of the surface. The images of droplets on the microstructured substrates were observed and evaluated by a CCD. Figure 1(c) is a 10 μL water droplet placed on the prepared superhydrophobic surface with the contact angle of 162°.

2.2 Measurement of dynamic contact angles and internal velocity distribution of water droplets

The strategy to measure the sliding angle and the contact angle hysteresis on each microstructured surface is to place a sessile droplet there and then to tilt the surface slowly until the droplet begins to slide. The angle subtended at the front of the droplet is the advancing contact angle (θ_A), whereas that at the rear is the receding contact angle (θ_R). The sliding behavior of the droplet on the inclined superhydrophobic surface was observed directly by recording dynamic images using a high-speed digital camera system mounted on contact angle meter, the advancing contact angle and the receding contact angle were measured from these pictures.

The internal velocity profiles of the water droplets were measured with a PIV system illustrated in Figure 2. The laser sheet from semiconductor laser (1500 mW intensity; 532 nm wavelengths) was focused on the meridian plane of the droplet on the inclined superhydrophobic substrates with micropillars. For PIV measurement, the 5 μL water droplet containing fluorescent particles (mainly polystyrene, 1 μm diameter, 1.05 g cm^{-3} density, 542 nm excitation wavelength, 612 nm emission wavelength, Duke Scientific Corp., CA, USA) was placed on the microstructured surface. The computer-controlled high speed camera (640 pixel × 480 pixel resolution at shutter speed of 400 fps) was used to obtain sequential images of the sliding motion of a water droplet on inclined superhydrophobic surfaces. The instantaneous velocity vectors in the water droplet were derived from two frames cross correlation, and the interrogation window was set to 32×32 pixels (streamwise×spanwise direction) and 75% overlap, so that the velocity vectors were obtained with 0.09 mm × 0.09 mm spatial resolution.

3 Results and discussion

3.1 Experimental results of microstructured surfaces

Figure 3 shows the measured static contact angle, advancing angle and receding angle of a 10 μL water droplet on micro-structured surfaces with different solid area fractions. Experimental results show that the static contact angle of water droplets on micro-structured surfaces increases as the solid area fraction decreases; this is in agreement with the predictions of the Cassie model [9]. Furthermore, we discovered that the advancing angle of water droplets on micro-structured surfaces was always maintained at approximately 162°, while the area fraction changes. However, the

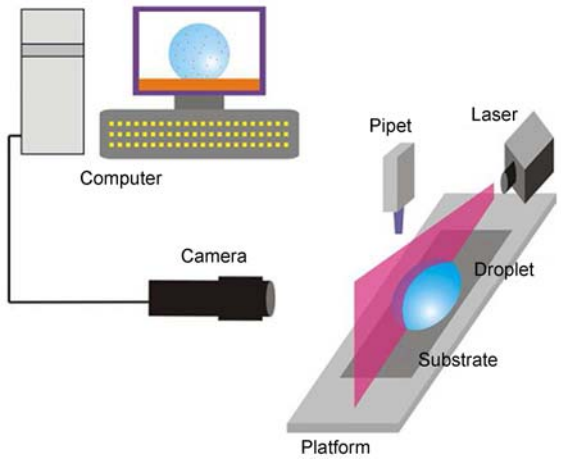

Figure 2 The schematics of the experimental setup used to reveal the internal flow field of the water droplet.

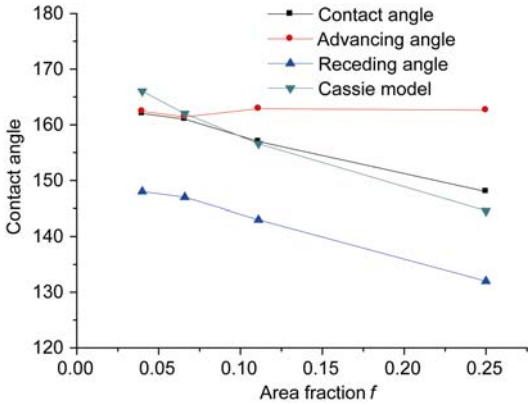

Figure 3 The static contact angle, advancing angle and receding angle of a 10 μL water droplet on micro-structured surfaces.

receding angle is closely related to the area fraction of the micro-structured surface, and visibly decreases with the increase in solid area fraction, resulting in the increase in contact angle hysteresis and roll-off angle. The resistance to the motion of a liquid droplet when it starts to roll off the surface primarily comes from the adhesive forces between the trailing edge of the liquid droplet and the microstructures. For the microstructured surface with regular micropillars array, the perimeter of contact line between the droplet and the solid surface increases with the solid area fraction of the microstructures. In other words, the larger the solid area fraction, the longer perimeter of contact line, and the stronger the adhesive forces between the water droplet and the solid surface. This is in agreement with available research findings [20,21].

We gently placed the water droplet on the micro-structured surface such that it was in a Cassie state, and then slowly increased the tilt angle of the micro-structured surface. When the angle of tilt of the solid surface is equal to the roll-off angle, the liquid droplet starts to move. Figure 4(a) shows the variation of the sliding distance of a 10 μL water droplet with respect to the time on a tilted micro-structured surface. Micro-structured surfaces with different solid area fractions have different roll-off angles ranging from 4° to 20°. We utilized the least squares method and differentiation to obtain the velocity and acceleration of the liquid droplet at different times. Experimental results show that at the initial stage (t<0.1 s), the velocity and acceleration of the liquid droplet are both very small, whereas the water droplet accelerates visibly when t>0.1 s. When the droplet slides on the inclined plane, the acceleration can be expressed as:

$$ma = mg\sin\alpha - F_{\text{hys}} - F_{\text{vis}}, \tag{1a}$$

or

$$a = g\sin\alpha - \frac{F_{\text{hys}} + F_{\text{vis}}}{m}, \tag{1b}$$

$$F_{\text{hys}} = \pi R_{\text{b}}\gamma_{\text{LV}}(\cos\theta_{\text{R}} - \cos\theta_{\text{A}}), \tag{2}$$

where α is the tilt angle. We can see from eq. (1), that the total resistance force $F_{\text{total}} = F_{\text{hys}} + F_{\text{vis}}$ comes from two sources: one is the hysteresis force F_{hys}, which comes from the hysteresis phenomenon between the droplet and the substrate; and the other is the viscous force F_{vis}, which comes from the hydrodynamic effect during the motion of the water droplet. Figure 4(b) shows the relationship between the total resistance and the solid area fraction. It is found that the total resistance force increased with the increasing of solid area fraction due to the larger contact angle hysteresis and viscous force on the boundary of the surface.

Figure 5 shows the variation of the advancing angle and receding angle of a 10 μL water droplet with respect to time as it slides down a micro-structured surface with 4 μm pillar width and 16 μm pillar spacing. During the initial stage of motion, the advancing angle and the receding angle of the water droplet are basically constant. An interesting observation is that the receding angle slowly increases with the increase in droplet velocity, whereas the advancing angle basically remains constant, resulting in the contact angle hysteresis slowly decreasing with the increase in droplet velocity. Throughout the entire sliding process, the average advancing angle of the water droplet on the micro-cylindrical structured superhydrophobic surface was 162.3°, the average receding angle was 149.5° and the average contact angle hysteresis was 12.8°.

In order to obtain the details of the internal flow of the droplet during the process of sliding, we used PIV to measure the internal flow field of the moving droplet. From the flow field shown in Figure 6(a), we found that a large proportion of the velocity vectors were of the same direction as the direction of sliding of the droplet. This shows that the motion of the droplet consists mainly of sliding, whereas rolling only takes place at the thin liquid layer at the

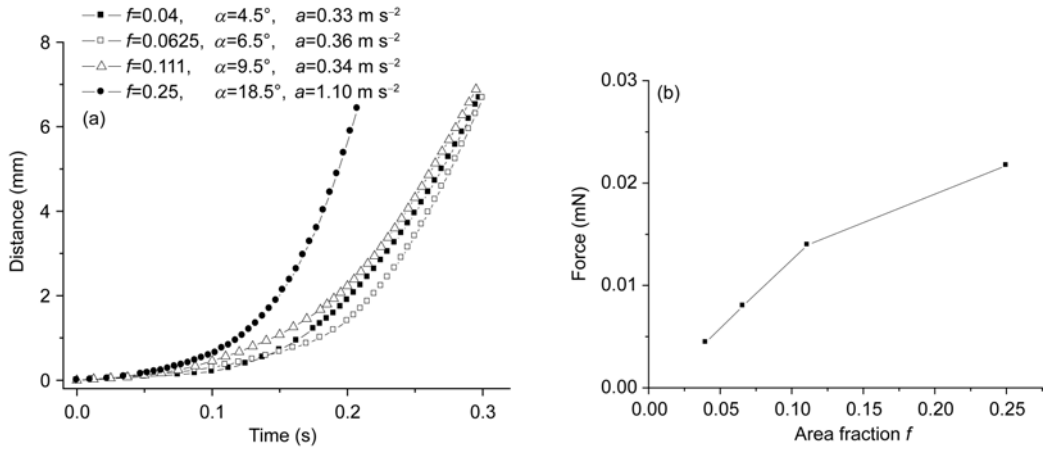

Figure 4 (a) Sliding distance vs. time of a 10 μL water droplet on microstructured substrates; (b) total resistance vs. solid area fraction of microstructured substrates.

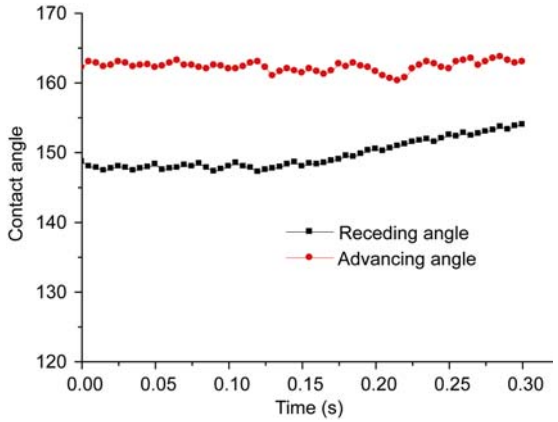

Figure 5 Dynamic contact angle of water droplets moving on a micro-structured surface.

edges of the droplet (Refer to ref. [22]). Figure 6(b) shows the variation with the height of the component of the droplet's velocity on the longitudinal centre line along the sliding direction of the droplet at different times. The experimental results show that near the solid surface, the flow velocity gradient is relatively large, whereas farther away from the surface, the velocity remains approximately constant, and can be thought of as the sliding of a rigid body. Thus, the shear force involved in the motion of the droplet is mainly concentrated on the area near the solid surface. Measurements of the velocity near the surface show that the velocity of the droplet at the surface is not zero, and that there exist visible sliding effects, whereby the sliding velocity is roughly 60% of the velocity of the centre of the droplet. The reason for this is that air pockets exist in the gaps within the microstructures of the solid surface, thus greatly decreasing the viscous shear effects between the solid surface and the liquid, thereby greatly decreasing the resistance to the motion of the droplet. These results are consistent with the experimental observations of the water droplet sliding on superhydrophobic surfaces by Sakai et al. [23–25].

3.2 Experimental results of the lotus leaf

There are numerous plants and animals in nature that have surfaces that are superhydrophobic (for example, the lotus leaf). In recent years, people have successfully created various biomimetic superhydrophobic surfaces by mimicking those surfaces found in nature. However, there is still very little research that has been done on the wetting properties of these superhydrophobic surfaces, with most research limited to the measurements of parameters such as the contact angle and contact angle hysteresis. There is still insufficient research with regards to the dynamic wetting behavior and motion characteristics of droplets on such superhydrophobic surfaces. This paper measures the dynamic contact angle and motion characteristics of water droplets on fresh lotus leaf surfaces, and compares these experimental results with the experimental results of water droplets on superhydrophobic surfaces with regular cylindrical microstructures.

First, we used a double-sided adhesive tape to stick the bottom surface of a small piece (15 mm × 8 mm) of a fresh lotus leaf on a smooth glass slide. We then used a burette to gently drip 10 μL of water on the surface of the lotus leaf and measured the contact angle. In our experiments, we measured the contact angles of droplets at 5 different positions on the same piece of a lotus leaf and took the average of these measurements. The result of this average measurement was 150°±3°. Due to the uneven distribution of the micro/nano-scale hair-like structures on the lotus leaf, the variation of the apparent contact angle at different positions on the leaf is rather large. We then placed the glass slide with the lotus leaf on a turntable, and slowly rotated the slide. The tilt angle of the surface, when the water droplet just slided from the lotus leaf, was recorded as the roll-off angle of the water droplet on the lotus leaf. The average roll-off angle value from three trials was 5°. Figure 7(b) shows the variation of the distance moved by the 10 μL water droplet with time on a superhydrophobic surface with cylindrical microstructures and on a lotus leaf. The roll-off

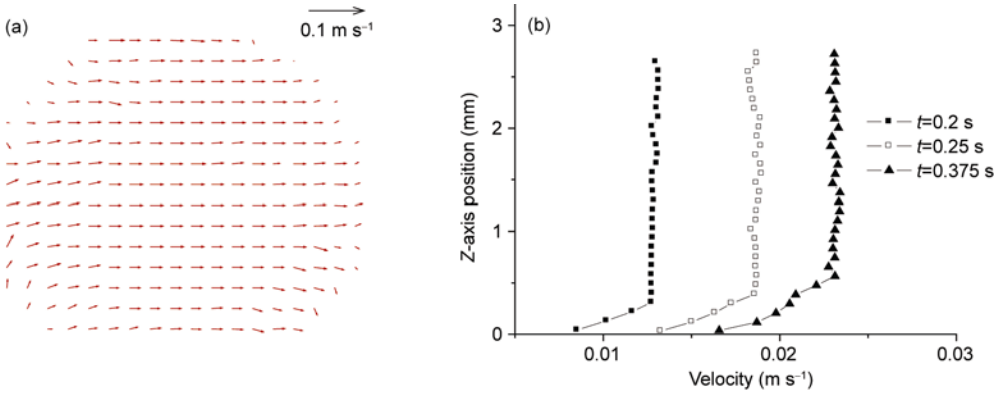

Figure 6 Internal flow field of a water droplet on a microstructured substrate with 4 μm pillar width and 16 μm pillar spacing: (a) distribution of the velocity vectors; (b) sliding velocity profiles vs. the *Z*-axis position.

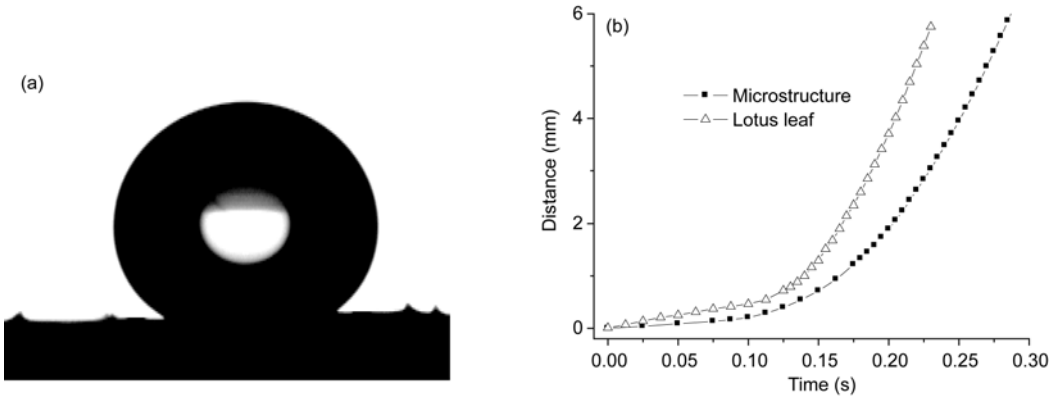

Figure 7 (a) A 10 μL water droplet on lotus leaf CA=152°; (b) sliding distance vs. time of a 10 μL water droplet on the microstructured substrate and lotus leaf.

angle of the water droplet on the superhydrophobic surface with micro pillars was 4.5°, and that of the lotus leaf was 5°; the two values are quite close. From Figure 7 we can see that for similar distances moved, the sliding velocity of the water droplet on the lotus leaf is faster than the sliding velocity of the water droplet on the superhydrophobic surface with microstructures. Using least squares fitting to a quadratic curve, we obtained the sliding acceleration (t>0.15 s) of a water droplet on a superhydrophobic surface with micro pillars to be 0.33 m s^{-2}, while the sliding acceleration (t>0.15 s) of a water droplet on a lotus leaf surface was 0.56 m s^{-2}.

From the angle of tile and the measured acceleration we can obtain the acceleration caused by resistive forces a_r ($a_r = g\sin\alpha - a$). The value a_r obtained from a water droplet on a superhydrophobic surface with micro pillars and on a lotus leaf were 0.44 and 0.29, respectively, showing that the resistive forces acting on a water droplet on a lotus leaf are smaller than the resistive forces acting on a water droplet on a superhydrophobic surface with cylindrical microstructures.

Figure 8 shows the variation with the time of the advancing angle and the receding angle of a 10 μL water droplet sliding down on a lotus leaf surface. When comparing this with Figure 5's results of the measurement of the dynamic contact angles of a water droplet on a superhydrophobic surface with micro pillars, we discovered that the amplitude of the variation of the advancing and receding angles of the water droplet on the lotus leaf was larger, and that situation in which the receding angle was larger than the advancing angle would exist. The reason for this is that a water droplet experiences a larger deformation when it moves over a taller neighboring tubercle structure on the lotus leaf. Experimental results also show that contact angle hysteresis for a water droplet sliding down a lotus leaf was smaller, and that during the entire sliding process, the average advancing angle of the water droplet on the lotus leaf was 150.5°, the average receding angle was 148° and the average contact angle hysteresis was 2.5°, far smaller than

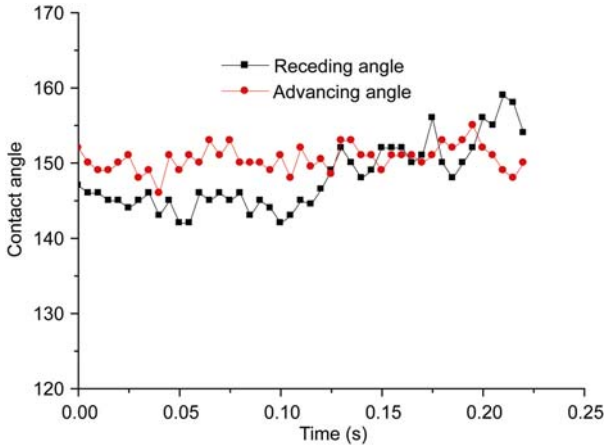

Figure 8 Dynamic contact angle of water droplets moving on a lotus leaf.

the contact angle hysteresis of a water droplet on a superhydrophobic surface with micro pillars. These experimental findings agree with existing experimental results [26,27], and show that even though the contact angle of a droplet on a lotus leaf is smaller when compared with a superhydrophobic surface with regular microstructures, the contact angle hysteresis of a water droplet sliding down a lotus leaf is far smaller than that of the super hydrophobic surface with surface structures on the micro-scale. In other words, a water droplet slides off a lotus leaf more easily, and thus the dynamic contact angle hysteresis is a better reflection of the dynamic wettability of a solid surface as compared with the apparent contact angle.

Figure 9 shows the internal flow fields of a water droplet sliding down a lotus leaf at different times, obtained by using PIV. Compared with the relatively smooth superhydrophobic surface with micro pillars, the surface roughness of the lotus leaf is greater, and there exist tubercle structures on a greater scale. A water droplet undergoes deformation when it passes over these obstacles, causing the internal flow directions of the water droplet to change at different times. In Figure 9(a), the direction of motion of the water

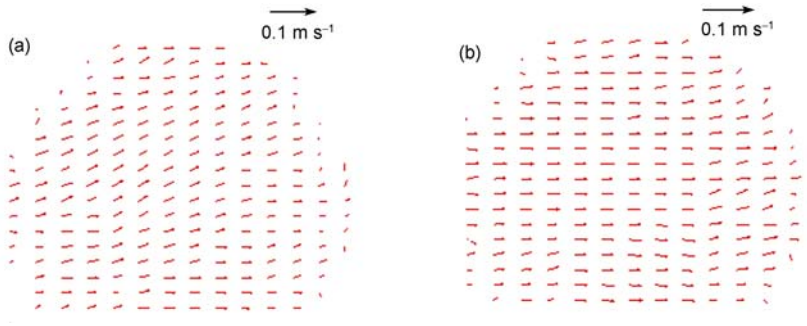

Figure 9 Internal flow fields of a 10 μL water droplet sliding down a lotus leaf. (a) t=0.15 s; (b) t=0.17 s.

droplet's centre portion points towards the upper right of the diagram, while at another instant, the direction of motion of the water droplet's centre portion is the same as the direction in which the water droplet is sliding (Figure 9(b)). As far as we know, there have not been any previous reports on the variation of the dynamic contact angle of a water droplet and measurements of the internal flow field as it slides down a lotus leaf.

Figure 10 presents the variation with the height of the component of the droplet's velocity on the longitudinal centre line along the sliding direction of the droplet at different times. The experiment results show that the component of the droplet's internal flow velocity along the direction of sliding of the droplet basically does not vary along the height of the droplet. This shows that a water droplet sliding down a lotus leaf can be approximated to a sliding of a rigid body, and that the shear deformation of the interior of the water droplet and between the water droplet and the lotus leaf surface is very small. Compared with the superhydrophobic surface with micro pillars, the water droplet sliding on the lotus leaf has a greater sliding velocity and experiences smaller resistive forces. This is in agreement with the previous measurements of the acceleration of a water droplet during the sliding process. Furthermore, recent research

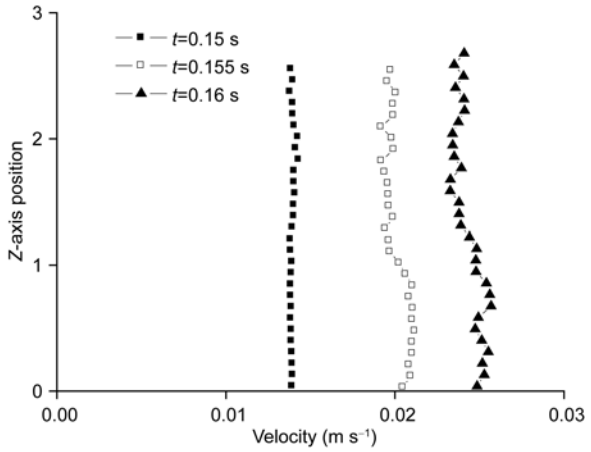

Figure 10 Internal flow fields of a 10 μL water droplet sliding down a lotus leaf.

on superhydrophobic materials has shown that, compared with monoscale micro- or nano-structured superhydrophobic surfaces, the resistive force experienced by a droplet when it flows over a multiscale micro/nano-structured surface is much less [28]. For a lotus leaf with multiscale micro/nanostructures, apart from having a smaller solid area fraction that allows air to remain in tiny gaps, the nano-scale hair-like structures on the micro-scale tubercles on the lotus leaf surface play a very important role in the formation of a stable gas-liquid interface. It can prevent nano water droplets from condensing on the lotus leaf surface, and can also prevent liquid from entering the gaps in the lotus leaf surface due to gas-liquid capillary waves and damaging the gas-liquid interface [29].

4 Conclusions

We measured the static contact angle, dynamic contact angle and acceleration of water droplets on an artificial superhydrophobic surface with regular micro pillars and on fresh lotus leaves. We also used particle image velocimetry (PIV) to measure the velocity distribution of liquid droplets on these superhydrophobic surfaces. The experimental results show that the dynamic contact angle of the water droplet varies as it slides down a superhydrophobic surface. Even though the static contact angle of a water droplet on a lotus leaf is smaller than the contact angle of a water droplet on a silicon wafer with regular micro pillars, the acceleration of a water droplet sliding down a lotus leaf is greater than the acceleration of a water droplet on a silicon wafer with microstructures. The reason for this is that the water droplet sliding down a lotus leaf has a smaller contact angle hysteresis and a large sliding velocity. Thus, compared with the static contact angle, the contact angle hysteresis and acceleration are more suitable parameters for evaluating the hydrophobicity of a material. Compared with monoscale micro-structured surfaces, the multiscale micro/nano-structures on a lotus leaf surface are advantageous in forming a stable gas-liquid interface, thus effectively reducing resistance to fluid flow.

The project was supported by the National Natural Science Foundation of China (Grant Nos. 11072126 and 10872106).

1 Hu D L, Chan B, Bush J W M. The hydrodynamics of water strider locomotion. Nature, 2003, 424: 663–666
2 Otten A, Herminghaus S. How plants keep dry: A physicist's point of view. Langmuir, 2004, 20: 2405–2408
3 Barthlott W, Neinhuis C. Purity of the sacred lotus, or escape from contamination in biological surfaces. Planta, 1997, 202: 1–8
4 Blossey R. Self-cleaning surfaces—virtual realities. Nat Mater, 2003, 2: 301–306
5 Parker A, Lawrence C. Water capture by a desert beetle. Nature, 2001, 414: 33–34
6 Eijkel J. Liquid slip in micro- and nanofluidics: Recent research and its possible implications. Lab Chip, 2007, 7: 299–301
7 Sanchez C, Arribart H, Guille M M G. Biomimetism and bioinspiration as tools for the design of innovative materials and systems. Nat Mater, 2005, 4: 277–278
8 Wenzel R N. Resistance of solid surfaces to wetting by water. Ind Eng Chem, 1936, 28: 988–994
9 Cassie A B D, Baxter S. Wettability of porous surfaces. Trans Faraday Soc, 1944, 40: 546–550
10 Onda T, Shibuichi S, Satoh N, et al. Super-water-repellent fractal surfaces. Langmuir, 1996, 12: 2125–2127
11 Wong T, Ho C M. Dependence of macroscopic wetting on nanoscopic surface textures. Langmuir, 2009, 25: 12851–12854
12 Furmidge C G L. Studies at Phase Interphases 1 Sliding of liquid drops on solid surfaces and a theory for spray for retention. J Colloid Sci, 1962, 17: 309–319
13 Miwa M, Fujishima A, Nakajima A, et al. Effects of the surface roughness on sliding angles of water droplets on superhydrophobic surfaces. Langmuir, 2000, 16: 5754–5760
14 Yoshimitsu Z, Nakajima A, Watanabe T, et al. Effects of surface structure on the hydrophobicity and sliding behavior of water droplets. Langmuir, 2002 18: 5818–5822
15 Nakajima A. Design of a transparent hydrophobic coating. J Ceram Soc Jpn, 2004, 112: 533–540
16 Yoshida N, Abe Y, Shigeta H, et al. Preparation and water droplet sliding properties of transparent hydrophobic polymer coating by molecular design for self-organization. J Sol Gel Sci Tech, 2004, 31: 195–199
17 Suzuki S, Nakajima A, Kameshima Y, et al. Elongation and contraction of water droplet during sliding on the silicon surface treated by fluoroalkylsilane. Surf Sci, 2004, 557: L163–L168
18 Song J H, Sakai M, Yoshida N, et al. Dynamic hydrophobicity of water droplets on the line-patterned hydrophobic surfaces. Surf Sci, 2006, 600: 2711–2717
19 Yoshida N, Abe Y, Shigeta H, et al. Sliding behavior of water droplets on flat polymer surface. J Am Chem Soc, 2006, 128: 743–747
20 Lv C J, Yang C Y, Hao P F, et al. Sliding of water droplets on microstructured hydrophobic surfaces. Langmuir, 2010, 26: 8704–8708
21 Dorrer C, Ruhe J. Advancing and receding motion of droplets on ultrahydrophobic post surfaces. Langmuir, 2006, 22: 7652–7657
22 Hao P F, Lv C J, Yao Z H, et al. Sliding behavior of water droplet on superhydrophobic surface. Eur Phys Lett, 2010, 90: 66003
23 Sakai M, Song J H, Yoshida N, et al. Direct observation of internal fluidity in a water droplet during sliding on hydrophobic surfaces. Langmuir, 2006, 22: 4906–4909
24 Suzuki S, Nakajima A, Sakai M. Rolling and slipping motion of a water droplet sandwiched between two parallel plates coated with fluoroalkylsilanes. Appl Surf Sci, 2008, 255: 3414–3420
25 Sakai M, Kono H, Nakajima A. Sliding of water droplets on the superhydrophobic surface with ZnO nanorods. Langmuir, 2009, 25: 14182–14186
26 Bhushan B, Koch K, Jung Y C. Fabrication and characterization of the hierarchical structure for superhydrophobicity and self-cleaning. Ultramicroscopy, 2009,109:1029–1034
27 Koch K, Bhushan B, Jung Y C, et al. Fabrication of artificial Lotus leaves and significance of hierarchical structure for superhydrophobicity and low adhesion. Soft Matter, 2009, 5: 1386–1393
28 Jung Y C, Bhushan B. Biomimetic structures for fluid drag reduction in laminar and turbulent flows. J Phys Condens Matter, 2010, 22: 035104